https://dx.doi.org/10.1016/j.coco.2021.100899

Carbon Nanotube-decorated Glass Fibre Bundles for Cure Self-monitoring and Load Self-sensing of FRPs

Yiyin Su[a], Lei Xu[a], Pengyu Zhou[a], Jianwei Yang[a], Kai Wang[b], Li-min Zhou[c], and Zhongqing Su[a,d,e*]

[a]Department of Mechanical Engineering
The Hong Kong Polytechnic University, Kowloon, Hong Kong SAR

[b]Department of Aeronautical and Aviation Engineering
The Hong Kong Polytechnic University, Kowloon, Hong Kong SAR

[c]School of System Design and Intelligent Manufacturing,
Southern University of Science and Technology, Shenzhen 518055, PR China

[d] The Hong Kong Polytechnic University Shenzhen Research Institute
Shenzhen 518057, P.R. China

[e] School of Astronautics, Northwestern Polytechnical University, Xi'an, 710072, P.R. China

Submitted to *Composites Communications*
(submitted on 12 June 2021; revised and re-submitted on 26 Jul 2021)

* To whom correspondence should be addressed. Tel.: +852-2766-7818, Fax: +852-2365-4703, Email: zhongqing.su@polyu.edu.hk (Prof. Zhongqing Su, *Ph.D.*)

Abstract

Extra to serving as the reinforcement in polymer-based composites, glass fibres (GFs) are decorated with dense and uniform carbon nanotubes (CNTs) via chemical vapor deposition at a low CNT growth temperature (500 ℃). The hairy CNT-decorated GF bundles measure the dynamic variation in electrical resistance using CNT-formed piezoresistive networks in the bundles, with which the resin flow front and cure progress of epoxy during fabrication are self-monitored by the composites. The bundles also precisely sense in-service loads applied to the composites, with a gauge factor as high as 30.2. Without intrusion to the original composites from sensors and sensor-associated electrodes/cables, the CNT-decorated GF bundles shed light on the use of nanocomposite-driven fibre decoration towards development of new functional composites.

***Keywords*:** fibre decoration; cure monitoring; nanocomposites; structural integrity monitoring; carbon nanotubes

1. Introduction

Load-bearing fibre-reinforced polymer composites (FRPs) are preferably functionalized with the capability of continuous, spontaneous monitoring of self-conditions from cure, through service to end of the life [1]. To accommodate such a demand, optical fibres and lead zirconate titanate (PZT) wafers are embedded in FRPs to gauge residual strains accumulated through manufacturing and external load-generated strains, to monitor the cure progress of matrix, or to characterize in-service damage [2, 3]. Even though, the sensors with an embeddable nature may degrade the original integrity of the host composite structures and lower the ultimate tensile strength up to ~10% [4, 5].

With recent advances in carbonaceous nanomaterials and carbon nanotubes (CNTs) in particular, introducing CNTs into FRPs bestows on the composites with somewhat unique yet intriguing functionality such as self-condition monitoring [6, 7]. CNTs can be either dispersed in polymer matrices or deposited on fibre surfaces [8-10], to form percolated CNT networks. The networks can respond to progressive change in cure condition, loads applied on FRPs, or material degradation due to the occurrence of damage, by calibrating variation in electrical properties of FRPs measured by the CNT networks. For direct dispersion, a challenging issue remains that the CNTs of high aspect ratio tend to entangle and/or aggregate one with the other, resulting in uneven dispersion of CNTs in polymer matrix and leading to downgraded responsivity and sensitivity of the CNT networks to changes in self-conditions of FRPs. Moreover, dispersing CNTs in matrix remarkably increases the viscosity of the matrix and gives rise to insufficient fabric infiltration, as a result of which voids are created in FRPs [11]. To circumvent such deficiency, CNTs are decorated on fibre surfaces via chemical vapor deposition (CVD) [12-14]. Decoration is conducive to the formation of dense, uniform CNT networks, with additional merits such as controllable CNT orientation and an enhanced weight loading of CNTs.

With such a motivation, in this study, glass fibres (GFs) are decorated with hairy CNTs via CVD at a low CNT growth temperature (500 ℃), to form CNT-decorated GF bundles in FRPs that are fabricated using a vacuum-assisted resin transfer molding (VARTM) technique. The morphology and quality of CNTs decorated on GFs are characterized. The CNT-decorated GF bundles, extra to serving as the reinforcement in polymer-based composites, enable continuous, spontaneous monitoring of self-conditions of FRPs, from cure through service, by measuring the dynamic variation in electrical resistance (ER) with CNT-formed piezoresistive networks in the bundles, without degrading the original integrity of FRPs due to sensor intrusion.

2. Materials and Methods

2.1 Material Preparation

Plain weave glass fibre fabrics (COLAN®, 175 gsm) are adopted as the reinforcement of the FRPs, while epoxy resin (WAM® ML-812A) and hardener (WAM® ML-812B) are mixed at a weight ratio of 2.5:1, as the matrix. To prepare the catalyst precursor solution, a stoichiometric amount of cobalt (II) nitrate hexahydrate (International Laboratory®) is dissolved in ethanol (Honeywell® 24194), with the mass concentration of 5.0 wt.%. The mixture is magnetically stirred for 2 h, with which the GF fabrics, as received form, are sufficiently impregnated. The thoroughly impregnated fabrics are then dried in an oven at 60 °C for 15 min.

With the catalyst precursor solution, CNTs grow on the cobalt nitrate hexahydrate-coated GF fabrics through a CVD process, schematically shown in **Fig. 1**. In this process, GF fabrics are inserted in a quartz tube attached to a furnace, in which an inert environment is maintained by purging the 5 vol% H_2/N_2 gas mixture (LINDE®) at 100 sccm for 2 h, prior to heating. The tube is heated at a rate of 10 ℃/min, and then kept at 450 ℃ for 30 min, to warrant full reduction of the catalyst precursor in the hydrogen-maintained atmosphere. The temperature continues to rise to 500 ℃, to initiate the growth of CNTs. The ethanol vapor at 85 ℃ is evaporated into the tube, to supply carbon source

for the synthesis of CNTs. The CNT growth lasts for 30 min, which has been proven sufficient to create hairy CNT-based piezoresistive networks on the fibre surfaces, yet not at the cost of sacrificing the mechanical strength of the fibres due to excessive exposure to the high temperature [12]. The H_2/N_2 gas mixture is continuously fed into the tube at a flow rate of 50 sccm during the entire CVD process, to facilitate CNT growth. The furnace is then cooled down to the room temperature with a rate of 10 ℃/min.

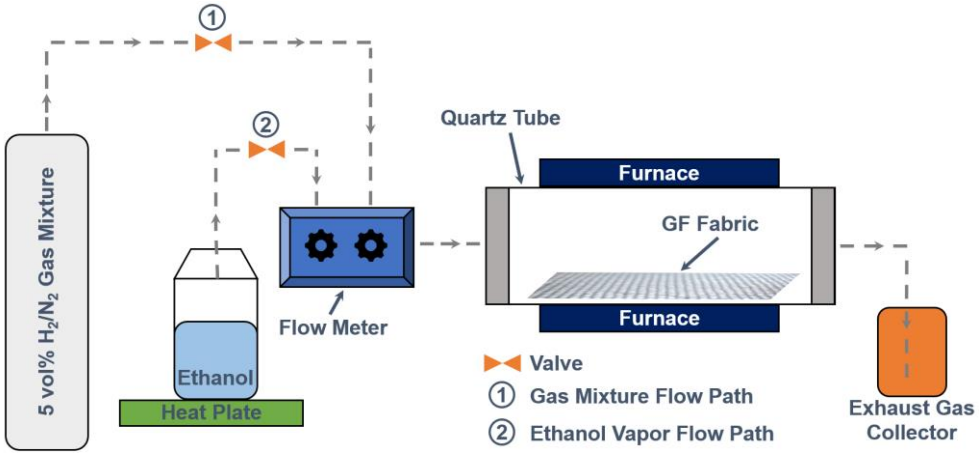

Fig. 1. Schematic of CNT growth on GF via CVD.

2.2 Morphological Characterization

A single GF filament that is decorated with CNT networks via the above CNT growth process is characterized using scanning electron microscopy (SEM, TESCAN® MAIA3) and transmission electron microscopy (TEM, JEOL® JEM-2100F), to characterize its morphology. Raman spectrum of the formed CNT networks is obtained with a Raman spectrometer (WITec® alpha300R) using a 532 nm laser as the excitation source. **Figure 2** shows the filament with highly dense and uniform CNT networks. A CNT growing on the GF filament is further scrutinized with TEM, revealing the co-axial, thin-walled tubular structure of the CNT, in **Fig. 3(a)**. The inner and outer diameters of the CNT measure ~12 nm and ~20 nm, respectively. With Raman spectroscopy, **Fig. 3(b)** confirms the graphitic structure of the CNT. Two distinct peaks are observed in the Raman spectrum, which

correspond to the D-band at ~1340 cm^{-1} and to the G-band at ~1580 cm^{-1} (owing to the crystallinity in the graphitic structure [15]), respectively. The I_D/I_G ratio is calculated to be ~0.88 in the spectrum, indicating a high degree of graphitization of the synthesized CNTs. The directly growing CNTs at a low temperature is a joint consequence of appropriate selection of hydrocarbon source, catalyst precursor and carrier gas, which differentiates this study from previous work.

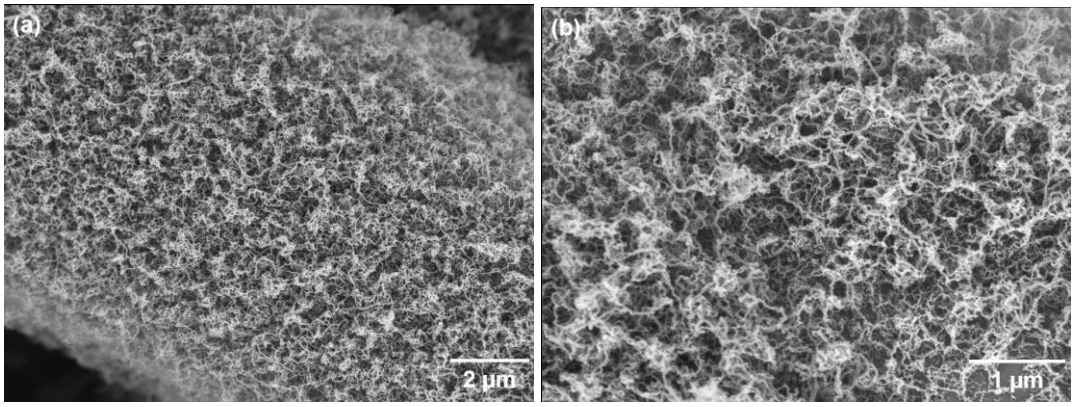

Fig. 2. SEM images of a GF filament with surface-decorated CNT networks (two scales).

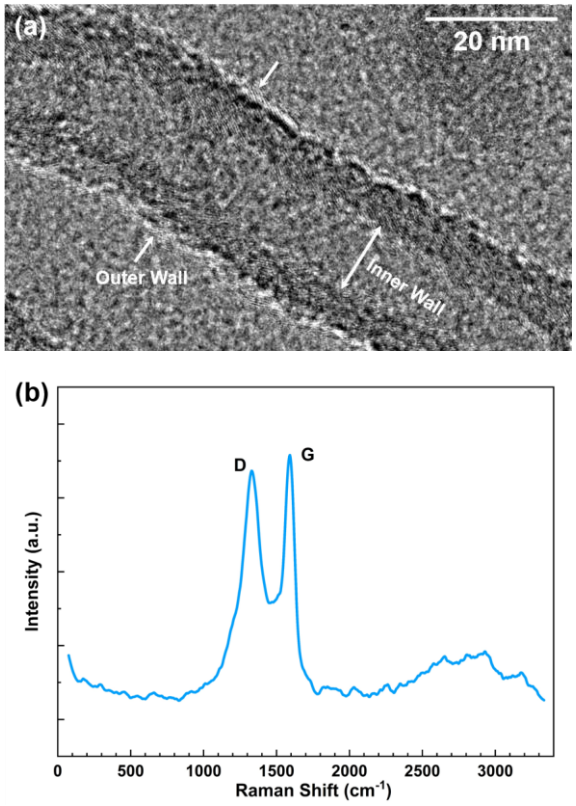

Fig. 3. (a) TEM image of a CNT decorated on a GF filament; and (b) Raman Spectrum of CNTs.

2.3 CNT-decorated-GF Bundles

With the above method, CNTs are initiated to grow on fibre surfaces in a specific region (120 × 10 mm^2) of a GF woven fabric, to form a bundle of GFs with decorated hairy CNT networks, and such CNT-decorated-GF bundles are referred to as *CNT-d-GFB* in what follows. A CNT-d-GFB in the fabric spans across the whole width of the fabric (to facilitate circuit connection). Such-made fabric layer is then inserted into another eight plies of GF fabrics during stacking, as the middle layer, to fabricate a 9-ply orthotropic GF laminate following a VARTM technique. In VARTM, a perforated peel ply and a flow mesh are added on the stacked fabrics. The CNT-d-GFB is circuited via a pair of electrodes (10 × 10 mm^2 each), as shown in **Fig. 4**. Externally connected, the electrodes and cables avoid intrusion to the laminate. To eliminate the effect of fluctuating pressure and temperature on ER measurement, a vacuum leak test is carried out prior to the infusion of resin, ensuring a constant pressure applied; and the preform is kept in a thermotank (25 ℃) through the entire infusion and cure processes, to remain a stable ambient temperature.

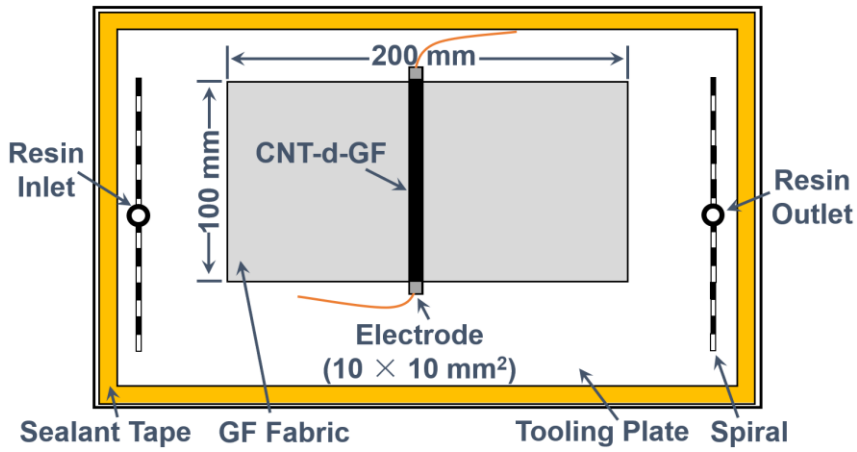

Fig. 4. Fabrication of a FRP laminate with a CNT-d-GFB via VARTM technique.

3. Results and Discussion

ER is measured real-time with the CNT-d-GFB using a digital graphical sampling multimeter (Keithley® DMM7510), from cure of the laminate to its use. The cure progress is calibrated in terms

of variation in ER, as detailed in **Section 3.1**; while ER is acquired when the laminate is subject to a tensile load, whereby to quantify the applied load, in **Section 3.2**. A standard strain gauge (120 Ω) is mounted on laminate surface to measure the load-induced strain, for comparison and calibration.

3.1 Cure self-monitoring

Figure 5 correlates the ER measured by the CNT-d-GFB with the status of epoxy cure through laminate fabrication. In **Fig (5)**, ΔR and R signify the variation in ER and the initial resistance of the CNT-d-GFB, respectively. In VARTM, the entire cure progress of epoxy embraces three sequential stages, namely: 1) the infusion stage – the injection of epoxy resin, to impregnate fabrics; 2) the equilibrium stage – the full infiltration of low-viscosity epoxy resin with fabrics, to infill dried spots and voids; and 3) the cure stage – the full consolidation of epoxy in the laminate. As observed,

1) in the infusion stage: the epoxy resin is quickly introduced to infuse both the fabrics and the CNT-d-GFB in the laminate, leading to a rapid increase in the measured ER, **Fig. 5(b)**. During this period, epoxy modules penetrate and expand CNT networks and remarkably alter the original nanostructure of the networks, as a result of which both the tunnelling resistance (due to a higher dielectric constant of matrix compared with that of air) and the contact resistance (due to the loss of contact among adjacent CNTs) of the CNT-d-GFB increase;
2) in the equilibrium stage which takes ~40 min: the progressive epoxy cure contributes to a high ER value, in **Fig. 5(c)**. This is attributable to the fact that after infilling the majority of the inter- and intra-roving voids in fabrics, the resin molecules continue to migrate into and interrupt the CNT networks, at a reduced speed owing to the barriers formed by the micro- or nano-scale dry voids within the CNT networks, leading to a mild increase in ER; and
3) in the cure stage: with continuous polymerization of epoxy as cure develops, the volume

shrinkage of epoxy resin becomes dominant, causing CNTs closer one to another. As a consequence, the ER measured by the CNT-d-GFB tends to decrease, as noted in **Fig. 5(d)**.

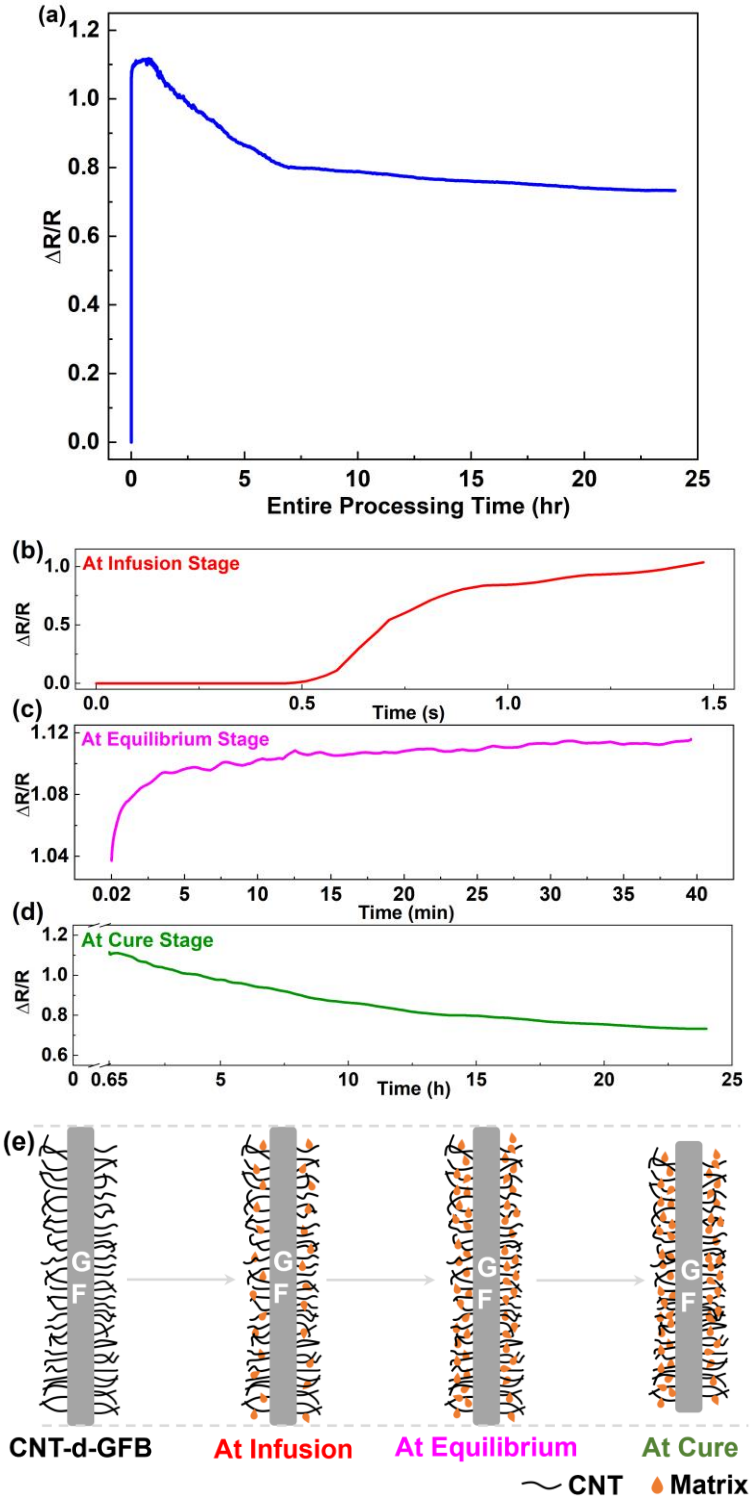

Fig. 5. Variation in ER measured by CNT-d-GFB in a VARTM process: (a) entire process; (b) infusion stage; (c) equilibrium stage; (d) cure stage; and (e) morphological alteration of CNT-d-GFB in different stages.

The above three cure stages, in which the CNT networks in CNT-d-GFB are morphologically altered as cure develops, are illuminated schematically in **Fig. 5(e)**. In terms of the ER measured by the CNT-d-GFB, the cure progress of FRPs can be monitored continuously.

3.2 Load Self-sensing

Upon full curing, the finished FRP laminate with CNT-d-GFB possesses the capability of self-sensing in-service loads. A series of tests under different loading conditions is conducted for validation. **Figure. 6** representatively shows the response of the laminate under a quasi-static tensile load (tensile rate: 3 mm/min) on a universal test platform (INSTRON® 5982). Within a strain scope of 0~1.5% (in an elastic deformation range of the laminate), the CNT-d-GFB-measured ER varies linearly against the load applied, in **Fig. 6**. To quantify the measurement sensitivity, a gauge factor (G) is defined as

$$G = \frac{\Delta R}{R_0 \cdot \varepsilon}, \quad \textbf{(1)}$$

where $\Delta R = R - R_0$ (R: the current resistance; R_0: the initial resistance), and ε the strain induced by the applied load. With **Eq. (1)**, G is calculated to be 30.2, which is remarkably higher than that of a standard strain gauge which is ~2.0 in general.

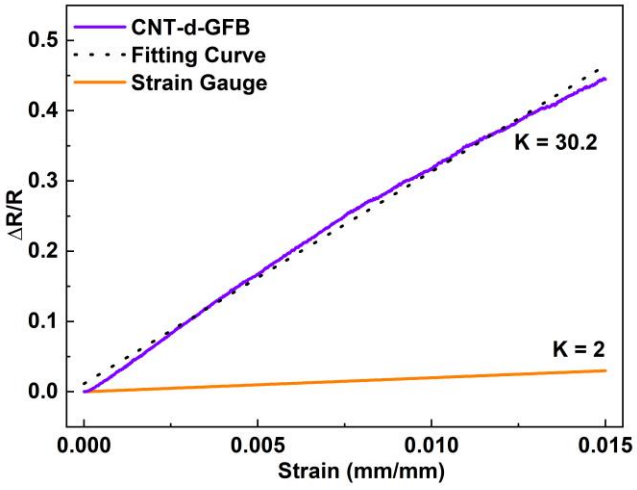

Fig. 6. Variation in ER measured by CNT-d-GFB when laminate is subject to a quasi-static load.

4. Conclusion

Glass fibre bundles, decorated with even and hairy CNT networks via chemical vapor deposition at a low CNT growth temperature (500 ℃), endow the host composite structures with the capacity of monitoring self-conditions from cure through service. ER measured by CNT-d-GFB is correlated with epoxy cure in three key stages during composite fabrication, whereby to implement cure self-monitoring. Thus-fabricated laminate with CNT-d-GFB also possesses the capability of self-sensing in-service loads, with a high gauge factor of 30.2. The synthesized CNT-d-GFB enables continuous, spontaneous condition and quality monitoring of FRPs, yet not at the cost of sacrificing the original integrity of composites due to possible intrusion from embedded sensors and sensor-associated electrodes/cables.

Acknowledgments

The work was supported by General Project (Nos. 51875492 and 12072141) and a Key Project (No. 51635008) received from the National Natural Science Foundation of China. Z Su acknowledges the support from the Hong Kong Research Grants Council via General Research Funds (Nos. 15202820, 15204419 and 15212417).

References

[1] C. Liu, Q. Fang, K. Lafdi, Novel wireless sensing design for composite durability study, Compos. Commun. 22 (2020) 100511.

[2] X. Liu, J. Li, J. Zhu, Y. Wang, X. Qing, Cure Monitoring and Damage Identification of CFRP using Embedded Piezoelectric Sensors Network, Ultrasonics (2021) 106470.

[3] X. Wang, G. Foliente, Z. Su, L. Ye, Multilevel decision fusion in a distributed active sensor network for structural damage detection, Struct. Health Monit. 5(1) (2006) 45-58.

[4] S. Mall, J. Coleman, Monotonic and fatigue loading behavior of quasi-isotropic graphite/epoxy laminate embedded with piezoelectric sensor, Smart Mater. Struct. 7(6) (1998) 822.

[5] Y. Su, J. Yang, Y. Liao, P. Zhou, L. Xu, L.-m. Zhou, Z. Su, An implantable, compatible and networkable nanocomposite piezoresistive sensor for in situ acquisition of dynamic responses of CFRPs, Compos. Sci. Technol. 208 (2021) 108747.

[6] Y. Wan, W. Hu, B. Yang, X. Zhao, G. Xian, Y. Yuan, L. He, C. Liu, J. Deng, On-line tensile damage monitoring of WGF/epoxy T-joint by the embedded MWCNT@ WGF sensor, Compos. Commun. 23 (2021) 100541.

[7] Y. Gola, D. Kim, S. Namilae, Piezoresistive nanocomposites for sensing MMOD impact damage in inflatable space structures, Compos. Commun. 21 (2020) 100375.

[8] B.N. Duc, Y. Son, Enhanced dispersion of multi walled carbon nanotubes by an extensional batch mixer in polymer/MWCNT nanocomposites, Compos. Commun. 21 (2020) 100420.

[9] K. Yildiz, İ. Gürkan, F. Turgut, F.Ç. Cebeci, H. Cebeci, Fracture toughness enhancement of fuzzy CNT-glass fiber reinforced composites with a combined reinforcing strategy, Compos. Commun. 21 (2020) 100423.

[10] Z. Wang, B. Yang, G. Xian, Z. Tian, J. Weng, F. Zhang, S. Yuan, X. Ding, An effective method to improve the interfacial shear strength in GF/CF reinforced epoxy composites characterized by fiber pull-out test, Compos. Commun. 19 (2020) 168-172.

[11] H. De Luca, D. Anthony, E. Greenhalgh, A. Bismarck, M. Shaffer, Piezoresistive structural composites reinforced by carbon nanotube-grafted quartz fibres, Compos. Sci. Technol. 198 (2020) 108275.

[12] A. Duongthipthewa, Y. Su, L. Zhou, Electrical conductivity and mechanical property improvement by low-temperature carbon nanotube growth on carbon fiber fabric with nanofiller incorporation, Compos. B. Eng. 182 (2020) 107581.

[13] J. Sebastian, N. Schehl, M. Bouchard, M. Boehle, L. Li, A. Lagounov, K. Lafdi, Health monitoring of structural composites with embedded carbon nanotube coated glass fiber sensors, Carbon 66 (2014) 191-200.

[14] D. He, B. Fan, H. Zhao, X. Lu, M. Yang, Y. Liu, J. Bai, Design of electrically conductive structural composites by modulating aligned CVD-grown carbon nanotube length on glass fibers, ACS Appl. Mater. Interfaces 9(3) (2017) 2948-2958.

[15] A.C. Ferrari, Raman spectroscopy of graphene and graphite: Disorder, electron–phonon coupling, doping and nonadiabatic effects, Solid State Commun. 143(1-2) (2007) 47-57.